Heliyon 7 (2021) e06003

Contents lists available at ScienceDirect

Heliyon

journal homepage: www.cell.com/heliyon

Research article

Chaga mushroom (*Inonotus obliquus*) polysaccharides exhibit genoprotective effects in UVB-exposed embryonic zebrafish (*Danio rerio*) through coordinated expression of DNA repair genes

Jehane Ibrahim Eid [a,*], Majdah Mohammad Al-Tuwaijri [b], Swabhiman Mohanty [c], Biswadeep Das [c,**]

[a] Department of Zoology, Faculty of Science, Cairo University, 12613, Egypt
[b] Department of Biology, Faculty of Applied Sciences. Umm Al-Qura University, Makkah, Saudi Arabia
[c] School of Biotechnology, KIIT University, Bhubaneswar 751024, India

ARTICLE INFO

Keywords:
Chaga polysaccharides
Zebrafish
UVB
DNA-Repair genes
Genotoxicity

ABSTRACT

Chaga mushroom is one of the promising beneficial mushrooms thriving in the colder parts of Northern hemisphere. Chaga polysaccharides (IOP) have been reported to enhance immune response and alleviate oxidative stress during development. However, the effects of IOP on the genotoxicity in model organisms are yet to be clarified. In this study, IOP was extracted using hot water extraction method, followed by GC analysis. Zebrafish embryos (12 h post fertilization, hpf) were exposed to transient UVB (12 J/m^2/s, 305–310nm) for 10 s using a UV hybridisation chamber, followed by IOP treatment (2.5 mg/mL) at 24 hpf for up to 7 days post fertilization (dpf). The genotoxic effects were assessed using acridine orange staining, alkaline comet assay, and qRT-PCR for screening DNA repair genes. Significant reduction in DNA damage and amelioration of the deformed structures in the IOP-treated zebrafish exposed to UVB ($p < 0.05$) was observed at 5 dpf and thereafter. The relative mRNA expressions of *XRCC-5, XRCC-6, RAD51,* and *GADD45* were significantly upregulated, whereas *p53* and *BAX* were downregulated in IOP-treated UVB-exposed zebrafish compared to UVB-exposed zebrafish. ELISA analysis revealed significantly decreased expression of XRCC5 and RAD51 in UVB-exposed compared to IOP-treated UVB-exposed and control zebrafish (7 dpf). However, p53 and BAX levels were high in UVB-exposed zebrafish, indicating higher apoptosis. Pathway analysis demonstrated coordinated regulation of DNA repair genes; p53 playing a pivotal role in regulating the expression of BAX, thereby promoting apoptosis in UVB-exposed zebrafish. Overall, IOP treatment ameliorated the genotoxic effects in UVB-exposed zebrafish by enhanced expression of DNA repair genes, which assisted in normal development. The study delineated the efficacy of IOP in mitigating UV-induced DNA damage in zebrafish.

1. Introduction

The surge for the development of natural products, including plants, marine organisms, and beneficial microorganisms has been intensified recently for drug and biosimilar discovery [1]. In this regard, Chaga (*Inonotus obliquus*) mushroom is one such biological product, which has gained attention worldwide, because of its medicinal values, including antioxidant, anti-inflammatory, antidiabetic, antiviral and many others [2, 3, 4, 5, 6, 7]. Chaga mushroom comprises a range of compounds, including polysaccharides, polyphenols, and triterpenes, which exhibit several health benefits. In particular, *I. obliquus* polysaccharide (IOP) represents the most active ingredient of Chaga mushroom, known for treating and preventing tumors, metabolic disorders, and many chronic diseases [5]. Besides, Chaga tea is also consumed in many countries for several remedies and health-promoting effects [5, 8]. Such beneficial effects are largely due to the immunomodulatory, anti-inflammatory and

* Corresponding author.
** Corresponding author.
E-mail addresses: jehaneeid@sci.cu.edu.eg (J.I. Eid), dviswadeep1983@gmail.com (B. Das).

https://doi.org/10.1016/j.heliyon.2021.e06003
Received 22 September 2020; Received in revised form 14 December 2020; Accepted 13 January 2021

anti-oxidative properties of *I. obliquus* polysaccharides, such as the branched polysaccharide β-glucan, which is one of the major polysaccharides found in IOP, and acts like a dietary fiber that greatly aids in digestion and absorption of nutrients, in addition to possessing anti-diabetic and anti-proliferative properties [3, 4, 5, 8].

DNA mutations are considered the main cause for cancer and genetic disorders. Hence, it is imperative to maintain the integrity of cellular DNA for proper development. Large-scale DNA damage can be deleterious to the cell and are caused by alkylating agents (transform a functional base into a mutagenic one), hydrolytic deamination (lead to base alterations), dyes (ethidium bromide), reactive oxygen species (intrinsic) and ionizing radiations (ultraviolet light, UV) [9, 10, 11]. UV light is one of the potent inducers of large scale DNA damage. UV light comprises three broad categories based on their wavelength: UVA (320–400 nm), UVB (290–320 nm), and UVC (240–290 nm). UVC is the most harmful to living organisms because of its high energy and is mostly absorbed by the stratospheric ozone [12, 13]. A part of UVB radiation is also absorbed in the stratosphere, though majority of UVB radiation reaches the earth's surface, and is responsible for serious health outcomes, such as skin cancer by inducing DNA damage. UVB results in two major types of mutagenic DNA lesions: cyclobutane–pyrimidine dimers, and pyrimidine adducts 6–4 photoproducts, in addition to their Dewar valence isomers [13].

Although there are in vivo repair mechanisms to manage and correct DNA mutations and maintain its integrity, such as photo-reactivation, base/nucleotide excision repair, DNA replication related methyl mismatch repair, in addition to large scale and nonspecific repair systems (SOS response and apoptosis), the degree of repair depends on the extent of damage and the status of the repair systems of the cell [12]. Therefore, intake of natural anti-oxidants and immune boosters are highly beneficial for maintaining a healthy body. In this regard, Chaga mushroom could be a potent beneficial product, whose benefits have been assessed in several metabolic and chronic disorders [4, 5, 8]. However, it is imperative to understand the effect of Chaga mushroom on the genotoxic profile in vivo to assess its effects on DNA damage.

Recently, many international toxicity researchers have utilized zebrafish (*Danio rerio*) as an in vivo model organism, because it possesses several measurable indicators in ecotoxicology, such as small size, high fecundity, well-characterized embryonic ontogenesis, transparent embryos, and rapid development [14]. Besides, zebrafish has more than 70% genome similarity with humans that render it to effectively model any human disease with high phenotypic similarity and convenience [15]. Zebrafish is an ideal model for assessing DNA damage and its counter mechanisms, because zebrafish genomic DNA contains DNA repair gene orthologues found in humans [14, 15]. In addition, zebrafish DNA is amenable to genetic manipulation using morpholinos, shRNA, or Crisprs [16]. UV-induced zebrafish models have also been developed to study the expression of DNA repair genes and tumor suppressor genes regulation [17, 18, 19]. Furthermore, transparent zebrafish casper mutants have been consistently used for tumor-related and toxicological studies for assessing the phenotypic manifestations during development [20]. Such avenues will be worthy to explore the expression of specific DNA repair genes that might play additional roles in embryological development. The objective of this study was to assess the molecular mechanism of IOP in UVB-exposed zebrafish during early development.

2. Materials and methods

2.1. Extraction of Chaga mushroom polysaccharides and GC-MSMS analysis

Extraction of Chaga mushroom polysaccharides (IOP) was performed using hot water-ethanolic extraction according to Eid et al., 2020 [14]. Briefly, 10 g of Siberian grade Chaga chunks were dried, ground to fine powder and dissolved in 150 mL distilled water followed by refluxing at 70 °C, vacuum dried and concentrated using 3 volumes of 95% ethanol. The solution was then centrifuged at 5000 rpm for 10 min, and the supernatant was dried and treated with Sevag reagent (chloroform:butanol in the ratio 4:1) to remove the proteins. The solution was then oven-dried and mixed with distilled water (5 g in 250 mL w/v), followed by chromatographic analysis and spectrophotometric confirmation [14].

GC-MS analysis was performed using trimethylsilylation reagent, TMS (N-Trimethylsilylimidazole) as per previous published protocol [14]. The monosaccharides were confirmed using internal standards and NIST library search. The area normalization method was employed to estimate the molar ratio of the monosaccharides present in the polysaccharide extract.

2.2. Zebrafish experiments

2.2.1. Embryo collection and UVB exposure

All the methods were approved and performed in accordance with the relevant guidelines and regulations of the Institutional Ethical Committee (IEC) of KIIT University. Zebrafish embryos were obtained from mating adult wild type zebrafish using a 2:1 female: male ratio, and the fertilized embryos were reared in embryo water (0.06% sea salt). Culture density of the fertilized embryos per mating was about 100. The fertilized embryos of 6-hour post-fertilization (hpf) were observed under microscope and pipetted in 6-well microplates for the exposure experiments. Zebrafish embryos at 12 hpf (n = 120), in the shield stage, were divided into three groups of 40 embryos each: Control, UVB-exposed, and IOP treated UVB-exposed groups. For UVB exposure and IOP treatment, the embryos (n = 80, 12 hpf) were exposed to UVB dose of 12 J/m^2/s using a UV cross linker hybridization chamber that emitted a range of 310–312 nm UVB light for 10 s. Then, the embryos were reared in embryo water at 28 °C. IOP treatment (2.5 mg/mL) was applied to half of the UVB-exposed embryos (n = 40, 24 hpf) that were labelled IOP-treated-UVB exposed group. The IOP concentration was selected based on our previous study that showed that the adopted dose did not affect the normal development of zebrafish embryos [14]. The embryos were grown for up to 7 days in the same medium and the fetal embryo toxicity and genotoxicity was assessed. The control group embryos were reared without any treatment in embryo water for the same duration. The assays were performed in duplicates. Morphological deformities based on phenotypic observations were recorded microscopically during embryonic development. The three zebrafish embryo groups were further assessed for genotoxicity assays using acridine orange staining, alkaline comet assay and qRT-PCR.

2.2.2. Acridine orange staining

Fluorescent acridine orange dye that binds to DNA and emits green fluorescence was used to stain the all the three groups at 5 dpf for qualitative assessment of the DNA damage. Briefly, control, UVB-exposed and IOP-treated (2.5 mg/mL)-UVB-exposed zebrafish embryos of 5 dpf (n = 10/group) were stained with 5 μg/mL acridine orange for 20 min, followed by washing the excess stain with embryo water. The corresponding images were captured in the GFP (green channel) of inverted fluorescent microscope (EVOS, Thermo Fischer Scientific, USA) to assess DNA damage (green dots represented apoptotic cells). The assays were performed in duplicates.

2.2.3. Alkaline comet assay for DNA damage analysis

DNA fragmentation is considered as one of the endpoints of genotoxicity. Genotoxicity was assessed by evaluating the DNA breaks using the alkaline comet assay and assessing the amount of DNA in the tail region (tail intensity). For this, control zebrafish, UVB-exposed zebrafish, and zebrafish treated with IOP (2.5 mg/mL) after UVB exposure were homogenized thoroughly in a micropestle in two independent experiments at 4 dpf and 7 dpf (n = 5/group). Then, 1 mL Dulbecco's Modified Eagle Medium (DMEM) with 10% FBS was added, and centrifuged for 5 min at 700 g at 15 °C. The pellet was retrieved and diluted in 1X PBS buffer pH 7.4 to form the cell suspension. Cell homogenate (10 μL) was

Table 1. Primers for the zebrafish genes used for the qRT-PCR.

Primer name	Primer (5′-3′)	Tm °C
BETA-ACTIN (F)	CGAGCAGGAGATGGGAACC	55
BETA-ACTIN (R)	CAACGGAAACGCTCATTGC	
XRCC5F	AGAAGTTTGTCCAGCGGCAGGTG	55.5
XRCC5R	GAGCATCGAGCCAGTCTGCCTG	
XRCC6F	TCGGAGAGGCTCTGTGGTGCT	56.5
XRCC6R	CTCCGGGCTTTGAGAGGTGCATC	
GADD45AF	CCTCAGTCATCCACATGGAAAG	56.5
GADD45AR	CAAACCCCGACTGTCTCTACAGA	
RAD 51 F	ACTAGCCGTCACCTGCCAGC	57
RAD 51 R	ACTGCCCACCAGACCATACCGTT	
BAX F	CCTTATCACCATCACCTCACTTC	57.5
BAX R	CCTTATCACCATCACCTCACTTC	
P53F	GGGCAATCAGCGAGCAAA	58
P53R	ACTGACCTTCCTGAGTCTCCA	

mixed with 0.8% low melting agarose and were dropped onto a glass slide precoated with normal melting agarose (1.5%), followed by covering with a cover slip. The slides were kept at 4 °C for 15 min for drying, followed by incubation in a cold lysis solution containing 100 mM EDTA, 2.5 M sodium lauryl sulphate, 1% Triton X-100, and 10% DMSO (pH 13.0) in the dark at 4 °C for overnight. Following incubation, the slides were dipped in a neutralizing solution containing 400 mM Tris at pH 7.4 for 30 min. Then, for assessing the unwinding of the DNA, electrophoresis was performed in a cold alkaline buffer (12 g/L NaOH and 0.37 g/L EDTA, pH 11) at 25V for 30 min. Post electrophoresis, the slides were washed in distilled water, and fixed with 70% ethanol for 5 min. Finally, the slides were stained with ethidium bromide (5 mg/mL) for 5 min and analyzed by fluorescence microscopy at 4X and 40 X magnifications (fluorescence at emission (500 nm) and excitation (530 nm) with an inbuilt image system (EVOS M5000, Thermo Fisher, USA). The images were analyzed using Image J analysis software for assessing the tail intensity in the three groups. The experiments were repeated for uniform analysis.

2.2.4. Gene expression analysis using qRT-PCR

Relative expression of DNA repair genes, *XRCC5, XRCC6, RAD51, GADD45*, *BAX,* and *P53* were assessed using Syber Green qRT-PCR. Beta actin was used as the reference gene. Briefly, total RNA was extracted independently from 5 dpf zebrafish larvae from the 3 groups [control, UVB-exposed and IOP-treated (2.5 mg/mL) UVB exposed] (n = 5/group) by using Trizol and converted to cDNA following standard protocol. cDNA was amplified using a Sybr-green based qRT-PCR master mix and specific primers (Table 1). The PCR thermal profile consisted of an initial denaturation of at 95 °C for 2 min, followed by 33 cycles of 30 s at 95 °C, 30 s at 55–62 °C (varied as per primers), and 30 s at 72 °C, and final extension at 72 °C for 3 min. Quantification and data analysis of the respective genes were assessed using the CFX manager of real-time PCR (Bio-Rad). The Ct values were calculated for each gene and were compared with the reference gene beta-actin, followed by estimation of ΔΔCt and fold change ($2^{-\Delta\Delta Ct}$) to assess the fold change in the gene expression among the different groups.

2.2.5. ELISA analysis

The expression of XRCC5, RAD51, P53 and BAX was assessed separately in 7 dpf zebrafish by Fish sandwich ELISA (My Bioresource, USA) using custom synthesized antibodies and TMB substrate. Briefly, 120 zebrafish embryos (7 dpf) previously exposed to UVB and IOP-treated as descried earlier were distributed between UVB-exposed and IOP-treated-UVB exposed groups (n = 60/group). Pools of 10 larvae/group were thoroughly homogenised in phosphate buffer saline, followed by centrifugation at 3000 rpm for 15 min, and the supernatant was used for ELISA analysis using the manufacturer's instructions. The absorbance was read at 450 nm after addition of stop solution and the concentration of the respective proteins were estimated from the standard curve.

2.3. Statistical analysis

The data obtained on the developmental characteristics, alkaline comet assay attribute, tail intensity (%), and the concentration of proteins after ELISA were analyzed using descriptive statistics in MS-Excel to obtain the mean ± standard deviation (SD). Protein expression levels

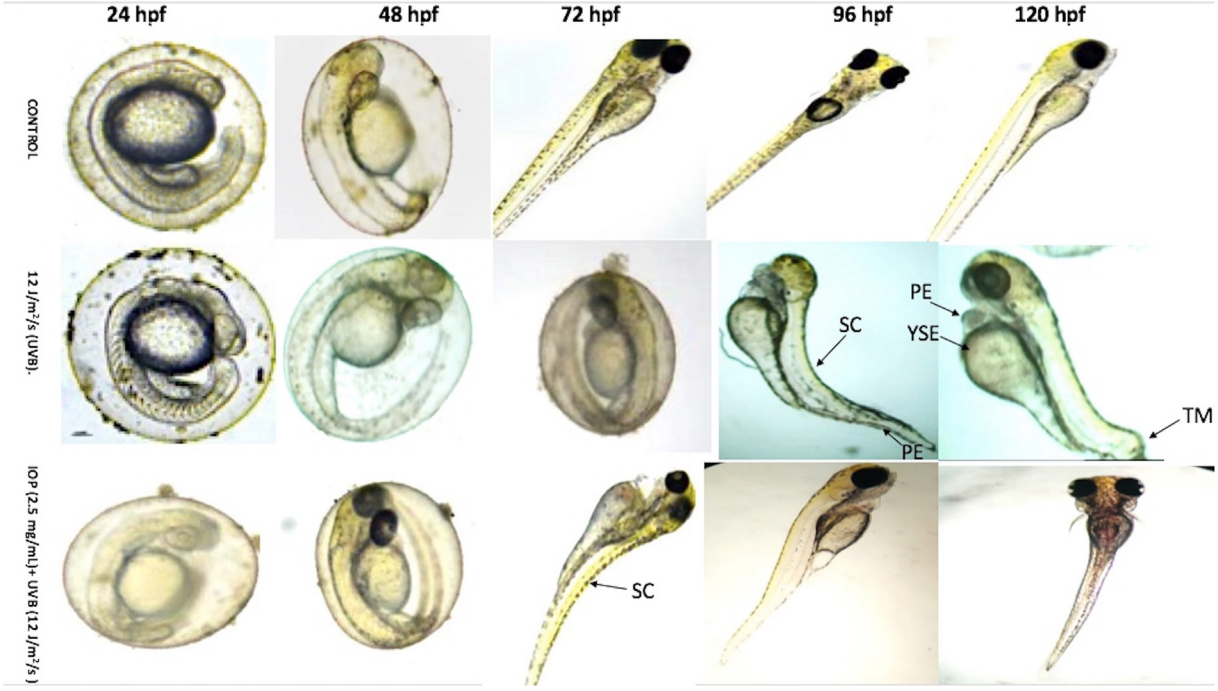

Figure 1. Bright field images of morphological analysis of zebrafish embryos (24 hpf to 120 hpf) in the three different zebrafish groups (control, UVB-exposed, IOP treated UVB-exposed). The structural deformities are shown in arrows: SC-spinal curvature, PE-pericardial edema, YSE-yolksac edema, TM-tail malformation.

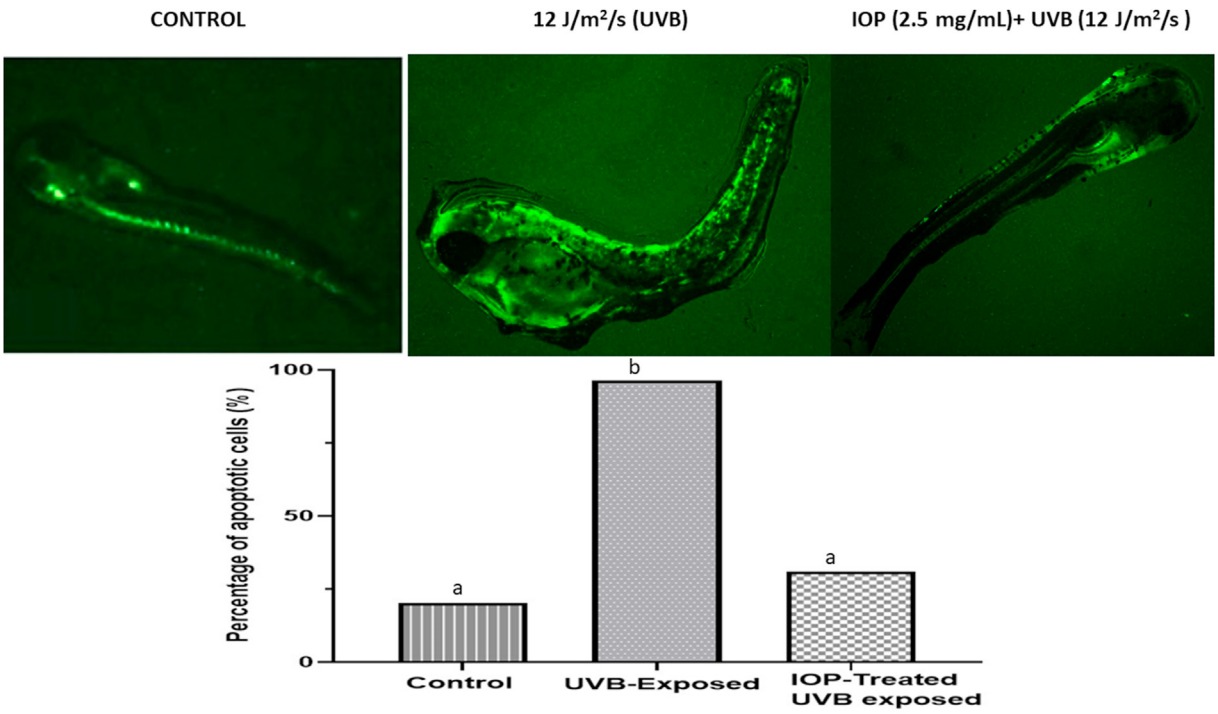

Figure 2. Acridine orange (AO) staining of zebrafish embryos (5 dpf): Above: Acridine orange staining pics for 5dpf zebrafish for the three groups; control, UVB-exposed, IOP treated UVB-exposed, showing intensive green fluorescence as significant uptake of AO dye due to cellular and DNA damage. Below: Histogram generated by Image J analysis showing the percentage of apoptotic cells in the three groups. Apoptosis was significantly high in the UVB-exposed group in comparison to control and IOP-treated UVB-exposed group. Different letters represent statistically significant differences (ANOVA, $P < 0.0001$).

after ELISA analysis among the IOP-treated UVB exposed and UVB-exposed groups were compared using unpaired Student T test. Relative gene expression for all the DNA repair genes was estimated with reference to the beta-actin gene in all the groups. Normality of the relative gene expression ($2^{-\Delta\Delta Ct}$) and the tail intensity of UV exposed zebrafish and IOP-treated UVB exposed group were determined using Shapiro Wilk test. The data was further compared between the groups using one-way analysis of variance (ANOVA) followed by post hoc analysis using Tukey HSD test, or non-parametric Kruskal Wallis test followed by Dunn test based on whether the data followed normal distribution or not. $P < 0.05$ was considered statistically significant for assessing the association of the variables in context to genotoxicity. The statistical tests were performed by importing the data from MS Excel into R studio Version 1.1.423, 2018.

3. Results

3.1. Developmental analysis upon IOP exposure in zebrafish embryos

Embryo development varied across the three groups; the UVB-exposed zebrafish showed several structural aberrations, such as yolk sac edema, organ deterioration involving eye, heart and tail regions, and slow development compared to control and IOP treated UVB-exposed groups (Figure 1). Average mortality was high in the UVB-exposed group (80%) during the course of development compared to IOP-treated (15%) and control (10%). Interestingly, IOP-treated UVB exposed group showed structural deformations like pericardial edema and spinal curvature in the early days of development (3 dpf), which were significantly ameliorated during late development (≥5 dpf) (Figure 1). The embryos remained healthy without showing any signs of mortality at the later stages of development in the IOP-treated group. The vital statistics such as development time, hatching rate and heart rate was similar in the control and IOP-treated UVB exposed group, which indicated that IOP promoted the development of zebrafish embryos as they would have developed under normal conditions. In addition, UVB-exposed fish showed significantly higher mean heart beat rate (heart rate = 204 ± 08 beats/min), delayed hatching (90% embryos did not hatch by 3 dpf) and slow development time.

3.2. Acridine orange staining

The level of DNA damage was assessed by the interaction of DNA binding AO dye, which was observed to be significantly uptaken by the UVB-exposed zebrafish embryos (5 dpf) compared to control and IOP-treated UVB-exposed groups. The uptake was visualized as intense green fluorescence, which was graphically represented as a histogram (Figure 2). Moreover, IOP-treated UVB-exposed group showed remarkably low green fluorescence demonstrating less DNA interactions with the dye. The results showed that IOP assisted in maintaining the integrity of the DNA, owing to less penetration of AO into the nucleus, which was similar to that in control embryos. These results indicated significantly increased apoptosis ($p < 0.05$) in the UV-exposed group without IOP exposure compared to IOP-treated UVB exposed group, which implied that IOP conferred protection against DNA damage.

3.3. Genotoxicity assessment using alkaline comet assay

Genotoxic assessment using the alkaline comet assay by analyzing the tail intensity in the three zebrafish groups revealed varying genotoxic effects, exhibiting distinct comet heads and tail regions (Figure 3). On 5 dpf, the tail intensity was significantly increased in the UVB-exposed zebrafish embryos by almost three-fold and four-fold compared to IOP-induced UVB exposed and control groups, respectively (Figure 4). On 7dpf, the tail intensity was further significantly increased in the UVB-exposed zebrafish embryos (86.6 %) by almost four-fold compared to

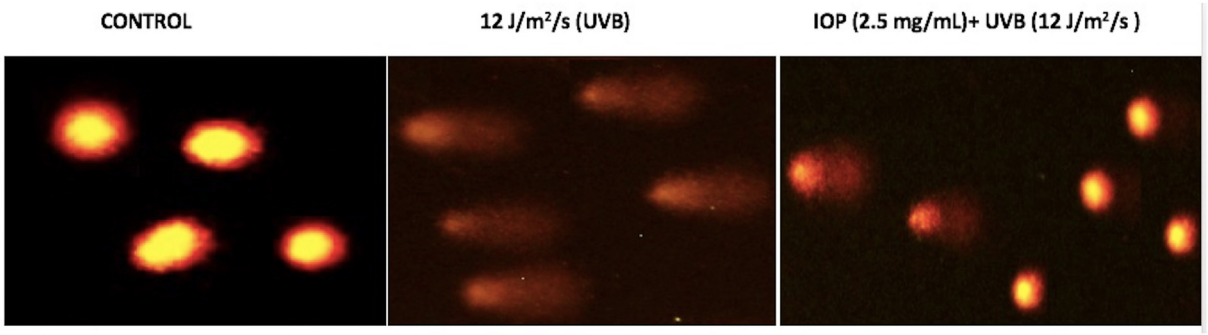

Figure 3. Alkaline comet assay showing distinct comet head and tail after ethidium bromide staining and fluorescent microscopy in the three zebrafish groups control, UVB-exposed, IOP treated UVB-exposed at 5dpf.

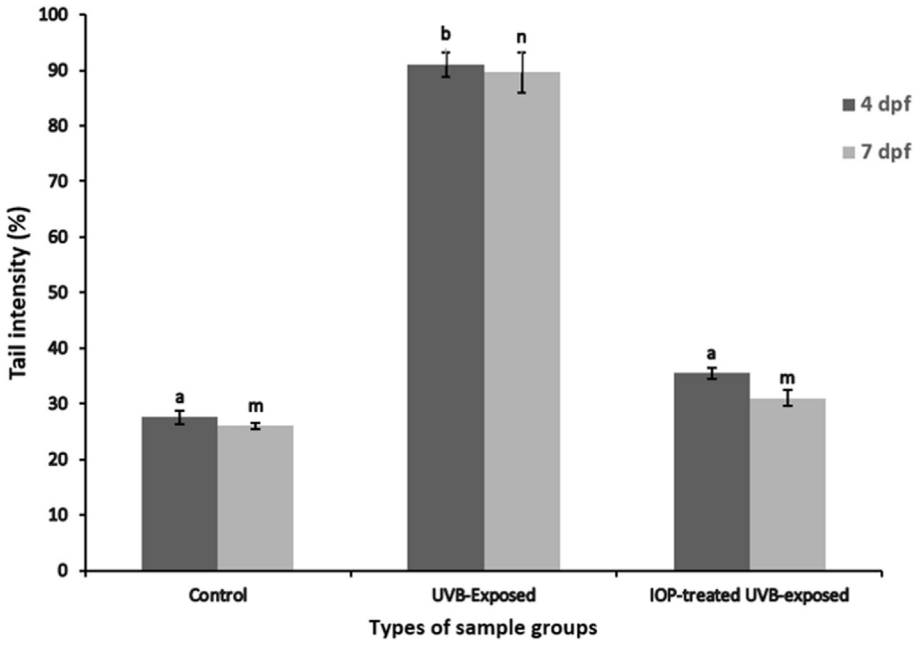

Figure 4. Comet assay histogram at 5 dpf and 7 pdf generated by analyzing the tail intensity (DNA fragmentation) using Image J in the three zebrafish (groups control, UVB-exposed, IOP treated UVB-exposed). Tail intensity was significantly increased in the UVB-exposed group compared to control and IOP-treated UVB exposed groups (ANOVA at 4dpf, $F = 2021$, $p < 0.0001$, ANOVA at 7 dpf $F = 2256$, $p < 0.0001$). Different letters represent statistically significant differences ($P < 0.05$).

both IOP-induced UVB exposed (32.1%) and control groups (26.1%), respectively (Figure 4). These results indicated that IOP acted as an anti-genotoxic compound, and assisted in the amelioration of genotoxicity caused due to UVB damage, thereby allowing the normal development of the zebrafish embryos.

3.4. Gene expression analysis upon IOP exposure in zebrafish embryos

qRT-PCR analysis showed that the relative expression of DNA repair genes *XRCC5, XRCC6, RAD51, GADD45,* and pro-apoptotic gene *BAX* was significantly different in the IOP-treated UVB-induced zebrafish and

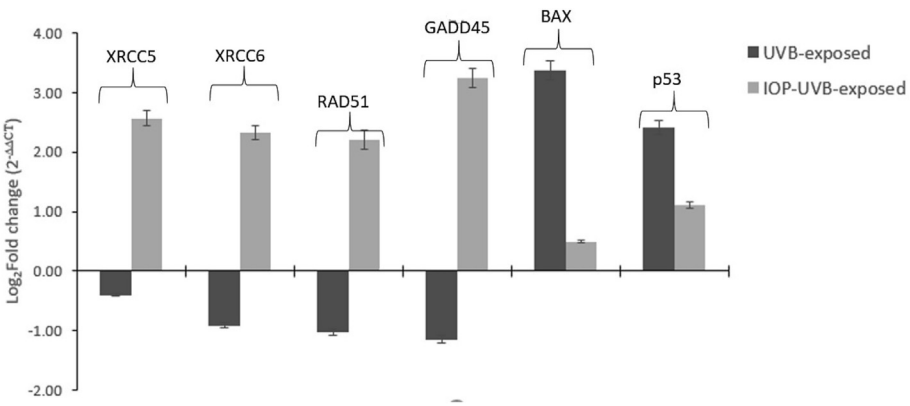

Figure 5. qRT-PCR bar graphs showing the $\log_2$ fold change in the gene expression in UVB-exposed and IOP-treated UVB exposed groups (5 dpf) compared to control (set at 0). Significant upregulation was observed in *GADD45, RAD51, XRCC5,* and *XRCC6* in the IOP-treated UVB-exposed group (Kruskal-Wallis test, $H = 32.31$, $p < 0.001$) compared to only UVB-exposed group. UVB exposed group showed significant upregulation of *p53* and *BAX* genes ($p < 0.0001$) that indicated enhanced apoptosis and cell death leading in zebrafish embryos.

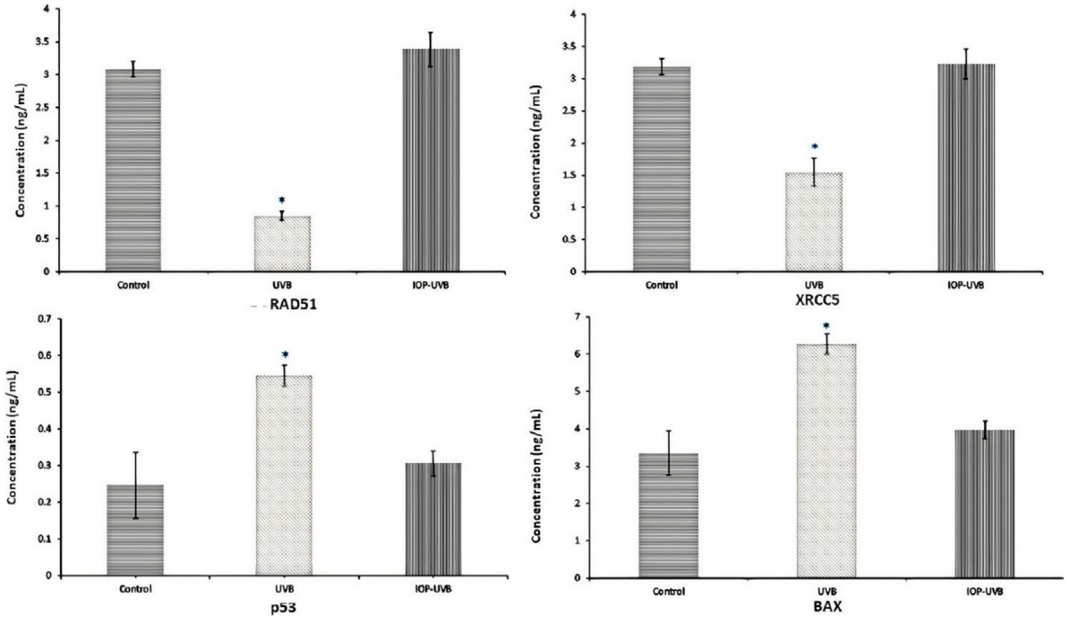

Figure 6. Sandwich ELISA analysis depicting the concentration of XRCC5, RAD51, p53, and BAX in control, UVB-exposed and IOP-UVB-exposed zebrafish larval pools (7 dpf, 10 larvae/pool/group). The levels of XRCC5 and RAD51 were significantly decreased inUVB exposed group compared to IOP-treated UVB-exposed group, whereas p53 and BAX levels were significantly increased in the UVB-exposed groups. Data is shown for a total of 120 zebrafish larvae/group. The readings were recorded in duplicates at 450 nm. * signifies a statistical significant value at $p < 0.05$.

UVB-exposed after normalization with the control groups ($p < 0.05$). Compared to control and IOP-treated UVB exposed group, the mean expression of *XRCC5, XRCC6, RAD51,* and *GADD45* was significantly lower in the UVB exposed zebrafish (Kruskal-Wallis test, $H = 32.31$, $p < 0.001$). In the UVB-exposed group, the mean expression of all the above-mentioned genes were downregulated compared to control and IOP-treated UVB exposed; except *p53* and *BAX (*increased by 3 fold*)* and *p53* (increased by 2.2 fold) compared to that of control zebrafish (Figure 5), which could indicate that UVB exposure induced substantial damage to the DNA repair system. The increased expression of *p53* and *BAX* gene in the UVB-exposed group increased apoptosis, leading to rapid cell death.

3.5. ELISA analysis

Sandwich ELISA results revealed significant differences in the expression of DNA repair proteins between UVB-exposed and IOP-treated UVB exposed groups. The expression of XRCC5, and RAD51 was significantly decreased in UVB exposed group compared to control and IOP-treated-UVB exposed group ($p < 0.05$) (Figure 6). However, the expression of p53 and BAX was high in UVB-exposed group compared to IOP-treated UVB-exposed group, which indicated enhanced apoptosis in UVB-exposed zebrafish. ELISA results corroborated with the qRT-PCR findings, which indicated that IOP enhanced the activity of DNA repair proteins, while enhancing apoptosis in UVB-induced zebrafish embryos.

4. Discussion

Mushrooms possessing medicinal values, such as Ganoderma, Chaga, *Agaricus* and many others have been consistently explored for health-promoting effects, because of their diverse benefits without inducing any undesirable effects [14, 15, 16, 17, 18, 19]. Besides, mushrooms are a rich source of natural bioactive compounds, and important biological elements, such as selenium, vitamin D, pantothenic acid, potassium and folic acid [20]. Previous studies have also reported the potential immunomodulatory and immunostimulatory effects of mushrooms, such as *Agaricus bisporus* in rainbow trouts, goldfish and zebrafish, which suggest that mushrooms can enhance the health and productivity of aquatic fish [21, 22, 23, 24]. We previously reported that IOP exposure in wild type zebrafish embryos promotes the growth and development and reduced the generation of intracellular ROS and oxidative stress, which further compelled us to assess its effects on the genotoxic profile in zebrafish [14]. In this study we assessed the effects of the widely known Chaga mushroom on the genotoxic profile in zebrafish and found that hot water extracted-Chaga polysaccharides significantly mitigated genotoxicity by enhancing the expression of DNA repair genes in UVB-induced zebrafish embryos. The IOP monomers revealed by GC analysis comprised certain unique sugars, including arabinose, xylulose, ribose, rhamnose, and glucose (Figure 7) that are known to be components of branched polysaccharides, such as β-glucan, which is reported to possess several health benefits [25]. β-glucan has been reported to have anti-diabetic, anti--proliferative properties, and anti-tumorigenic properties [26]. Such beneficial effects could be attributed to the ability of β-glucan to scavenge free radicals generated due to endogenous or exogenous agents, such as ionizing UVB radiation, thereby assisting the cells to repair DNA [27]. Several studies have reported that β-glucan readily facilitates the reduction of both simple and complex chromosomal aberrations, and confers protection to DNA against single-strand and double-strand breaks [28], in addition to enhancing the DNA repair system [29]. Hence, β-glucan confers protection to DNA through its antioxidant activity and by enhancing the DNA repair system. Recently, several bioactive polysaccharides isolated from natural sources have been given much attention in clinical pharmacology [20, 21, 29]. Such polysaccharides can be modified by chemical methods to improve the antitumor activity of polysaccharides and their clinical qualities, such as water solubility. Therefore, IOP could be regarded as a potential adjunct along with conventional therapeutics for several ailments that have wide applications in clinical settings [30, 31].

The present study revealed that continuous exposure to IOP reversed the structural deformations that were induced due to UVB exposure in zebrafish embryos. Severe organ damage and loss of vital structures, such as heart inflammation, structural abnormalities of the head regions, eyes deformation, and tail degradation, which occurred in the UVB-exposed zebrafish were significantly ameliorated in the IOP-treated UVB induced group (Figure 1). This suggested that IOP conferred protection to the zebrafish embryos against exogenous agents.

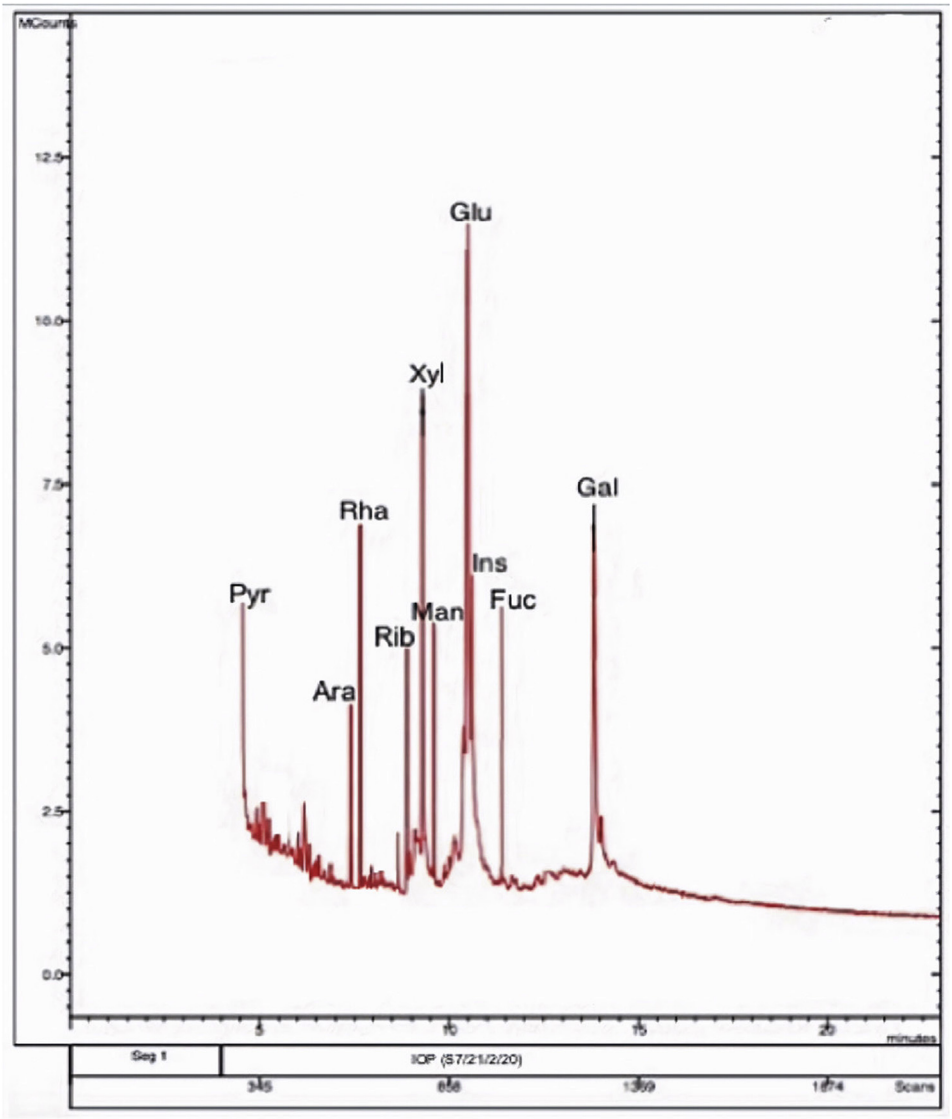

Figure 7. GC-MS chromatogram depicting the retention time peaks for different monomers of Chaga mushroom polysaccharides after hot water ethanolic extraction.

During early development, DNA damage results in severe structural deformations, which was observed in the UVB-exposed zebrafish. The reversal of such damage and eventual normal development of the zebrafish embryos could be solely attributed to continuous exposure to IOP that can be further explained due to the presence of high amount of beta-glucans and other beneficial components [31, 32, 33, 34]. Moreover, we observed the reversal of DNA damage by comet assay as the comet tail intensity was significantly reduced in the IOP-treated UVB-exposed group. This suggested that IOP was anti-genotoxic and conferred protection to DNA by maintaining its integrity. Furthermore, IOP reduced the number of apoptotic cells in the zebrafish embryos as demonstrated by acridine orange staining, whereas apoptosis was significantly increased in UVB-exposed zebrafish. This could be correlated with increased expression of the Bcl2 associated X gene, *BAX* that promoted apoptosis in UVB-exposed zebrafish. Furthermore, increased expression of *p53* along with *BAX* gene in UV-induced zebrafish implied enhanced apoptosis, because BAX expression is primarily governed by p53 [30]; hence, increased p53 expression will enhance the stimulation of pro-apoptotic protein BAX that will cause early cell death in UVB-exposed group. In addition, the downregulation of p53 and BAX in IOP-treated group indicated mitigation of p53-BAX apoptosis in the developing embryos, which suggested that IOP inhibited apoptosis and increased cellular longevity in zebrafish embryos.

Continuous exposure to IOP significantly reduced the amount of damaged DNA and thus, the embryos developed normally. Such DNA protective effects could be explained by the enhanced expression of several DNA repair genes. In this study, we observed significantly increased expression of *XRCC5, XRCC6, RAD51*, and *GADD45* genes in IOP-treated UVB-exposed group compared to UVB-exposed group. *XRCC5* and *XRCC6* encode Ku70 and Ku80 DNA repair proteins that function collectively during non-homologous end joining during DNA damage. Increased expression of these genes have also been reported in several disorders involving DNA damage to correct the DNA [35, 36]. *RAD51* encodes a protective enzyme that facilitates the repair of double strand DNA breaks by catalyzing strand transfer between a broken sequence and its undamaged homologue to allow re-synthesis of the damaged region [37, 38]. It has a major role in homologous recombination, and assists in recombination repair during extensive DNA damage [38]. Increased expression indicated prompt recruitment of DNA repair proteins for the correction of damaged DNA, and maintaining its integrity during early development. We also found increased expression of *GADD45* gene, which encodes the growth arrest and DNA damage proteins that have a critical role during embryogenesis by regulating differentiation (by inducing the zygotic gene expression) along with protecting DNA from spontaneous damage, mainly by efficient recognition and repair of spontaneous DNA damages by ten-eleven translocation

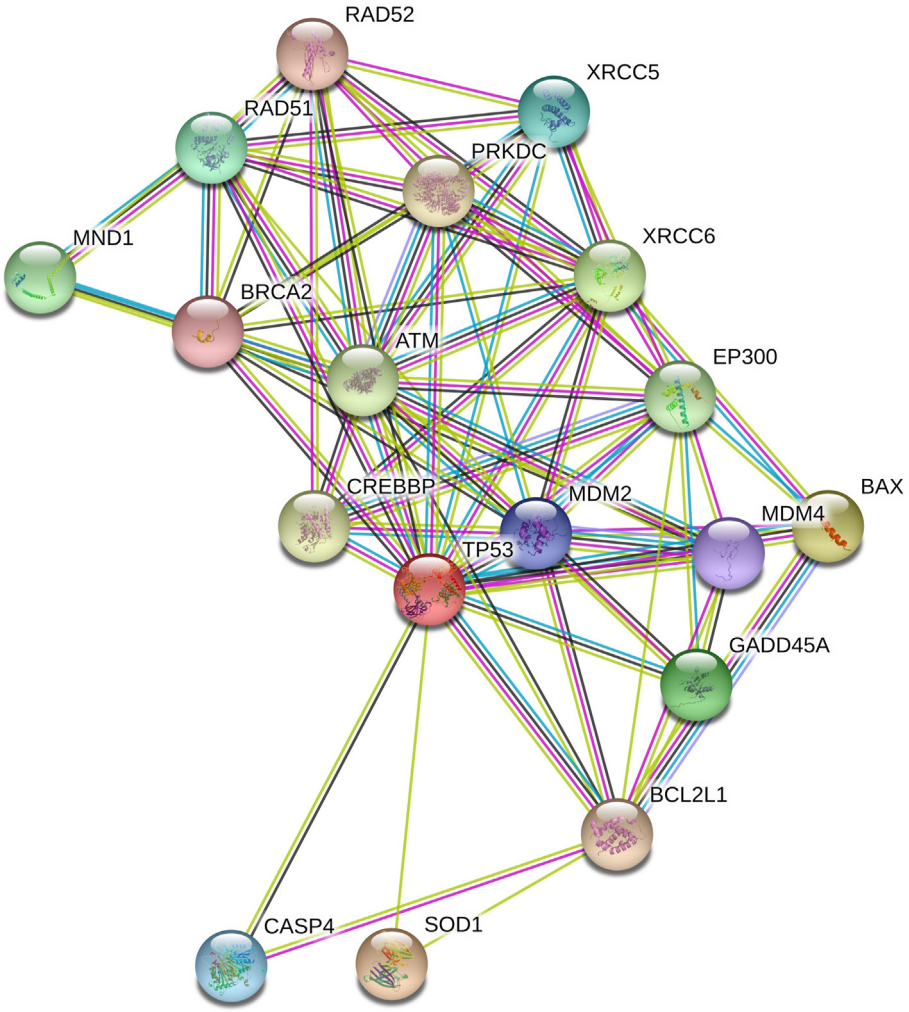

Figure 8. Network analysis using String software demonstrating the coordinated association of the DNA repair genes involved during UV induced DNA repair. DNA repair genes such as *RAD51, XRCC5, XRCC6,* and *GADD45* acted collectively and were involved in coordinate expression. p53 was the central player involved in inducing the expression of pro-apoptotic gene, *BAX*.

methylcytosine dioxygenase 1 (TET)-mediated DNA demethylation [39, 40, 41, 42]. This gene was highly expressed in IOP-treated UVB-exposed group, which suggested that IOP greatly enhanced the expression of *GADD45* proteins that eventually assisted the embryos in normal development. Network analysis showed that all the DNA repair genes acted in a coordinate manner during cellular signaling against DNA damage. Furthermore, *p53* acted as the central player regulating the coordinate response of all the genes involved in DNA repair and pro-apoptotic gene *BAX* (Figure 8).

In vivo developmental analyses showed that continuous exposure to IOP extract did not exhibit any significant developmental deformities in embryonic zebrafish, which developed in line with control embryos. The findings of this study suggested that Chaga mushroom aided in the normal development of the zebrafish embryos and reduced DNA damage in the developing embryos upon UVB exposure. Chaga mushroom can be regarded as a genoprotective agent and its efficacy can be explored further in clinical conditions.

5. Conclusion

Chaga mushroom polysaccharides exhibited genoprotective effects in zebrafish embryos exposed to UVB radiation. The polysaccharides comprised combination of unique sugars that caused amelioration of DNA damage leading to normal development in zebrafish. Chaga mushroom polysaccharides further enhanced the expression of DNA repair genes *XRCC-5, XRCC-6, RAD51,* and *GADD45,* which were coordinately regulated, suggesting collective response during UVB-induced DNA damage. In addition, the expression of *p53* and *BAX* genes were reduced upon IOP treatment, thereby indicating the amelioration of apoptosis, promoting cellular longevity. Overall, Chaga polysaccharide treatment ameliorated the genotoxic effects in UVB-exposed zebrafish, and assisted in normal development. The findings uncovered the benefits of Chaga mushroom on DNA damage and advocated its use and development as a natural therapeutic.

Declarations

Author contribution statement

J. I. Eid: Conceived and designed the experiments; Performed the experiments; Analyzed and interpreted the data; Contributed reagents, materials, analysis tools or data; Wrote the paper.

M. M. Al-Tuwaijri: Analyzed and interpreted the data; Contributed reagents, materials, analysis tools or data.

S. Mohanty: Performed the experiments.

B. Das: Conceived and designed the experiments; Performed the experiments; Analyzed and interpreted the data; Wrote the paper.

Funding statement

This research did not receive any specific grant from funding agencies in the public, commercial, or not-for-profit sectors.

Data availability statement

Data included in article/supplementary material/referenced in article.

Declaration of interests statement

The authors declare no conflict of interest.

Additional information

No additional information is available for this paper.

Acknowledgements

We are thankful to Mr. Sayam Ghosal and Ms. Agnihotri Panda, KIIT University, for assisting with GC analysis and in result interpretation for the work.

References

[1] A.G. Atanasov, B. Waltenberger, E.M. Pferschy-Wenzig, T. Linder, C. Wawrosch, P. Uhrin, V. Temml, L. Wang, S. Schwaiger, E.H. Heiss, et al., Discovery and resupply of pharmacologically active plant-derived natural products: a review, Biotechnol. Adv. (2015).

[2] C. Chen, W. Zheng, X. Gao, X. Xiang, D. Sun, J. Wei, C. Chu, Aqueous extract of Inonotus bliquus (Fr.) Pilat Hymenochaetaceae) significantly inhibits the growth of Sarcoma 180 by inducing apoptosis, Am. J. Pharmacol. Toxicol. (2007).

[3] S.H. Lee, H.S. Hwang, J.W. Yun, Antitumor activity of water extract of a mushroom, Inonotus obliquus, against HT-29 human colon cancer cells, Phyther. Res. (2009).

[4] Z. Li, J. Mei, L. Jiang, C. Geng, Q. Li, X. Yao, J. Cao, Chaga medicinal mushroom inonotus obliquus (Agaricomycetes) polysaccharides suppress tacrine- induced apoptosis by reactive oxygen species-scavenging and mitochondrial pathway in hepg2 cells, Int. J. Med. Mushrooms (2019).

[5] L. Ma, H. Chen, P. Dong, X. Lu, Anti-inflammatory and anticancer activities of extracts and compounds from the mushroom Inonotus obliquus, Food Chem. (2013).

[6] Jehane Eid, Biswadeep Das, Molecular insights and cell cycle assessment upon exposure to Chaga (*Inonotus obliquus*) mushroom polysaccharides in zebrafish (*Danio rerio*), Sci. Rep. 10 (7406) (2020).

[7] Jehane Eid, Majdah Al-Tuwaijri, Chaga mushroom (Inonotus Obliquus) inhibits growth of lung adenocarcinoma (A549) cells but not aspergillus fumigatus, Curr. Topics Nutraceutical. Res. 16 (4) (2018) 289–296.

[8] T. Vitak, B. Yurkiv, S. Wasser, E. Nevo, N. Sybirna, Effect of medicinal mushrooms on blood cells under conditions of diabetes mellitus, World J. Diabetes (2017).

[9] C.L. Bladen, D.J. Kozlowski, W.S. Dynan, Effects of low-dose ionizing radiation and Menadione, an inducer of oxidative stress, alone and in combination in a vertebrate embryo model, Radiat. Res. (2012).

[10] A.R. Collins, Investigating oxidative DNA damage and its repair using the comet assay, Mutat. Res. Rev. Mutat. Res. (2009).

[11] D.L. Mitchell, D. Karentz, The induction and repair of DNA photodamage in the environment, in: Environmental UV Photobiology, 1993.

[12] C.F. Errol, C.W. Graham, S. Wolfram, D.W. Richard, A.S. Roger, E. Tom, DNA Repair and Mutagenesis, second ed., 2006.

[13] J.H. Yoon, C.S. Lee, T.R. O'Connor, A. Yasui, G.P. Pfeifer, The DNA damage spectrum produced by simulated sunlight, J. Mol. Biol. (2000).

[14] J.J. Zhang, Y. Li, T. Zhou, D.P. Xu, P. Zhang, S. Li, H. Li, Bin bioactivities and health benefits of mushrooms mainly from China, Molecules (2016).

[15] M. Jayachandran, J. Xiao, B. Xu, A critical review on health promoting benefits of edible mushrooms through gut microbiota, Int. J. Mol. Sci. (2017).

[16] G. Ma, W. Yang, L. Zhao, F. Pei, D. Fang, Q. Hu, A critical review on the health promoting effects of mushrooms nutraceuticals, Food Sci. Hum. Wellness (2018).

[17] U. Lindequist, T.H.J. Niedermeyer, W.D. Jülich, The pharmacological potential of mushrooms. *Evidence-based Complement*, Altern. Med. (2005).

[18] A. Géry, C. Dubreule, V. André, J.P. Rioult, V. Bouchart, N. Heutte, P. Eldin de Pécoulas, T. Krivomaz, D. Garon, Chaga (inonotus obliquus), a future potential medicinal fungus in oncology? A chemical study and a comparison of the cytotoxicity against human lung adenocarcinoma cells (A549) and human bronchial epithelial cells (BEAS-2B), Integr. Cancer Ther. (2018).

[19] T.Y. Vitak, S.P. Wasser, E. Nevo, N.O. Sybirna, Structural changes of erythrocyte surface glycoconjugates after treatment with medicinal mushrooms, Int. J. Med. Mushrooms (2015).

[20] H. Van Doan, S.H. Hoseinifar, M.Á. Esteban, M. Dadar, T.T. Thu, Mushrooms, seaweed, and their derivatives as functional feed additives for aquaculture: an updated view, in: Studies in Natural Products Chemistry, 2019, pp. 41–90.

[21] O. Amiri, H.K. Miandare, S.H. Hoseinifar, A. Shabni, S.R. S, Skin mucus protein profile, immune parameters, immune-related gene expression, and growth performance of rainbow trout (Oncorhynchus mykiss) fed white button mushroom (Agaricus bisporus) powdered, Int. J. Med. Mushrooms 20 (2018) 337–347.

[22] R. Safari, S.H. Hoseinifar, S. Nejadmoghaddam, M. Dadar, Combined administration of the white button mushroom Agaricus bisporus (agaricomycetes) and lactobacillus casei modulated immune-related gene expression and mucosal and serum immune parameters in a goldfish (Carassius auratus) model, Int. J. Med. Mushrooms 21 (2019) 503–513.

[23] R. Safari, S.H. Hoseinifar, M. Dadar, M. Khalili, Powder of the white bottom mushroom, Agaricus bisporus (Agaricomycetes), improved immunomodulatory and health-promoting effects of lactobacillus casei in zebrafish (Danio rerio), Int. J. Med. Mushrooms 20 (2018) 695–704.

[24] S.H. Hoseinifar, H.K. Zou, H. Paknejad, A. Hajimoradloo, H. Van Doan, Effects of dietary white-button mushroom powder on mucosal immunity, antioxidant defence, and growth of common carp (Cyprinus carpio), Aquaculture 501 (2019) 448–454.

[25] J. Wang, W. Hu, L. Li, X. Huang, Y. Liu, D. Wang, L. Teng, Antidiabetic activities of polysaccharides separated from Inonotus obliquus via the modulation of oxidative stress in mice with streptozotocin-induced diabetes, PloS One (2017).

[26] Y.C. Sim, J.S. Lee, S. Lee, Y.K. Son, J.E. Park, J.E. Song, S.J. Ha, E.K. Hong, Effects of polysaccharides isolated from Inonotus obliquus against hydrogen peroxide-induced oxidative damage in RINm5F pancreatic cells, Mol. Med. Rep. (2016).

[27] C. Wang, R.K. Santhanam, X. Gao, Z. Chen, Y. Chen, C. Wang, L. Xu, H. Chen, Preparation, characterization of polysaccharides fractions from Inonotus obliquus and their effects on α-amylase, α-glucosidase activity and H2O2-induced oxidative damage in hepatic L02 cells, J. Funct. Foods (2018).

[28] T.G. Pillai, P. Uma Devi, Mushroom beta glucan: potential candidate for post irradiation protection, Mutat. Res. Genet. Toxicol. Environ. Mutagen (2013).

[29] T.G. Pillai, C.K.K. Nair, K.K. Janardhanan, Polysaccharides isolated from Ganoderma lucidum occurring in Southern parts of India, protects radiation induced damages both in vitro and in vivo, Environ. Toxicol. Pharmacol. (2008).

[30] S.N. Upadhyay, B.S. Dwarakanath, T. Ravindranath, T.L. Mathew, Chemical radioprotectors, Def. Sci. J. (2005).

[31] J.J. Volman, J.P.F.G. Helsper, S. Wei, J.J.P. Baars, L.J.L.D. van Griensven, A.S.M. Sonnenberg, R.P. Mensink, J. Plat, Effects of mushroom-derived β-glucan-rich polysaccharide extracts on nitric oxide production by bone marrow-derived macrophages and nuclear factor-κb transactivation in Caco-2 reporter cells: can effects be explained by structure? Mol. Nutr. Food Res. (2010).

[32] Y.W. Kim, K.H. Kim, H.J. Choi, D.S. Lee, Anti-diabetic activity of β-glucans and their enzymatically hydrolyzed oligosaccharides from Agaricus blazei, Biotechnol. Lett. (2005).

[33] B. Du, Z. Bian, B. Xu, Skin health promotion effects of natural Beta-Glucan derived from cereals and microorganisms: a review, Phyther. Res. (2014).

[34] V. De Oliveira Silva, R.V. Lobato, E.F. Andrade, C.G. De Macedo, J.T.C. Napimoga, M.H. Napimoga, M.R. Messora, R.M. Murata, L.J. Pereira, β-Glucans (Saccharomyces cereviseae) reduce glucose levels and attenuate alveolar bone loss in diabetic rats with periodontal disease, PloS One (2015).

[35] B.J. Sishc, A.J. Davis, The role of the core non-homologous end joining factors in carcinogenesis and cancer, Cancers (Basel) (2017).

[36] B.C. Gomes, S.N. Silva, A.P. Azevedo, I. Manita, O.M. Gil, T.C. Ferreira, E. Limbert, J. Rueff, J.F. Gaspar, The role of common variants of non-homologous end-joining repair genes XRCC4, LIG4 and Ku80 in thyroid cancer risk, Oncol. Rep. (2010).

[37] H.M. Chow, K. Herrup, Genomic integrity and the ageing brain, Nat. Rev. Neurosci. (2015).

[38] R.S. Bindra, P.J. Schaffer, A. Meng, J. Woo, K. Maseide, M.E. Roth, P. Lizardi, D.W. Hedley, R.G. Bristow, P.M. Glazer, Down-regulation of Rad51 and decreased homologous recombination in hypoxic cancer cells, Mol. Cell Biol. (2004).

[39] R.A. Donnianni, Z.X. Zhou, S.A. Lujan, A. Al-Zain, V. Garcia, E. Glancy, A.B. Burkholder, T.A. Kunkel, L.S. Symington, DNA polymerase delta synthesizes both strands during break-induced replication, Mol. Cell (2019).

[40] J.H. Lee, T.T. Paull, ATM activation by DNA double-strand breaks through the Mre11-Rad50-Nbs1 complex, Science (80-) (2005).

[41] J.A. Hackett, M. Azim Surani, DNA methylation dynamics during the mammalian life cycle, Philos. Trans. R. Soc. B Biol. Sci. (2013).

[42] J.-K. Zhu, Active DNA demethylation mediated by DNA glycosylases, Annu. Rev. Genet. (2009).

Update

Heliyon

Volume 7, Issue 6, June 2021, Page

DOI: https://doi.org/10.1016/j.heliyon.2021.e07235

Heliyon 7 (2021) e07235

Contents lists available at ScienceDirect

Heliyon

journal homepage: www.cell.com/heliyon

Corrigendum

Corrigendum to "Chaga mushroom (Inonotus obliquus) polysaccharides exhibit genoprotective effects in UVB-exposed embryonic zebrafish (Danio rerio) through coordinated expression of DNA repair genes" [Heliyon 7 (2) (February 2021) Article e06003]

Jehane Ibrahim Eid [a,*], Majdah Mohammad Al-Tuwaijri [b], Swabhiman Mohanty [c], Biswadeep Das [c,**]

[a] Department of Zoology, Faculty of Science, Cairo University, 12613, Egypt
[b] Department of Biology, Faculty of Applied Sciences. Umm Al-Qura University, Makkah, Saudi Arabia
[c] School of Biotechnology, KIIT University, Bhubaneswar 751024, India

In the original published version of this article, an incorrect version of Figure 7 was provided. This has now been corrected. The correct version of Figure 7 can be found below.

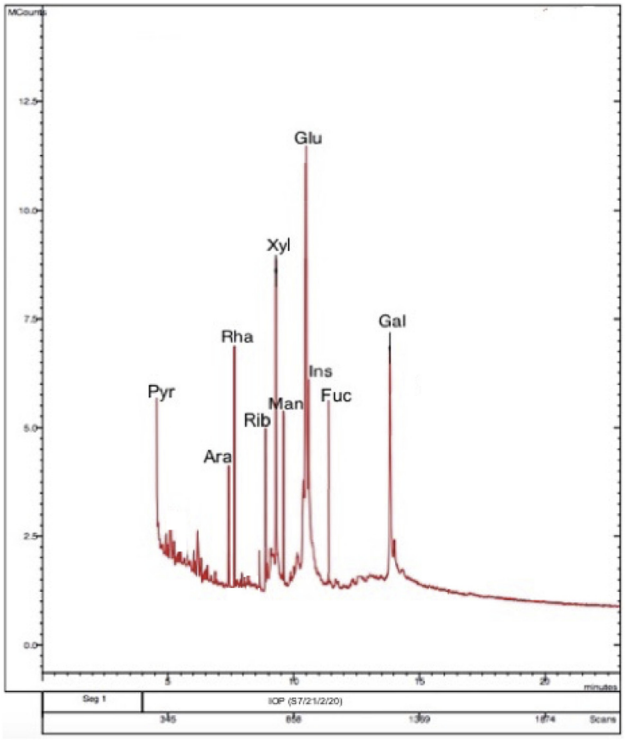

The authors apologize for the errors. Both the HTML and PDF versions of the article have been updated to correct the errors.

DOI of original article: https://doi.org/10.1016/j.heliyon.2021.e06003.
* Corresponding author.
** Corresponding author.
E-mail addresses: jehaneeid@sci.cu.edu.eg (J.I. Eid), dviswadeep1983@gmail.com (B. Das).

https://doi.org/10.1016/j.heliyon.2021.e07235
Received 2 June 2021; Accepted 2 June 2021